Advanced Materials Science and Technology Vol 4 Issue 2 2022
DOI: 10.37155/2717–526X–0402–4

ORIGINAL RESEARCH ARTICLE

Open Access

Omniscient Pte.Ltd.

Build Redox Composite Electrode Materials Based on Polymerized Redox Ionic Liquids

Yachao Zhu[1], Jie Deng[2], Olivier Fontaine[3,*]

[1]ICGM, Universsité de Montpellier, CNRS, ENSCM, Montpellier 34095, France.
[2]Institute for Advanced Study & College of Food and Biological Engineering, Chengdu University, Chengdu 610106, China.
[3]Molecular Electrochemistry for Energy Laboratory, School of Energy Science and Engineering, Vidyasirimedhi Institute of Science and Technology (VISTEC), Rayong 21210, Thailand.

***Correspondence to:** Olivier Fontaine, Molecular Electrochemistry for Energy Laboratory, School of Energy Science and Engineering, Vidyasirimedhi Institute of Science and Technology (VISTEC), Rayong 21210, Thailand. Email: olivier.fontaine@vistec.ac.th

Received: September 7, 2022; **Accepted:** November 19, 2022; **Published Online:** November 30, 2022

Citation: Zhu Y, Deng J, and Fontaine O. Build Redox Composite Electrode Materials Based on Polymerized Redox Ionic Liquids. *Advanced Materials Science and Technology*, 2022;4(2):049387.
https://doi.org/10.37155/2717-526X-0402-4

Abstract: Electrochemists are racing to develop new organic and inorganic materials for batteries and supercapacitors. As Organic Radical Battery technology approaches, a wide variety of materials are being proposed. However, devising materials with both ionic conductivity and redox storage properties is a strategy to be explored. In this paper, we show a new composite based on mixing carbon nanotubes and redox ionic liquids. The present work's originality is that this composite is realized for the first time and allows a couple of different types of conduction/storage: electronic conduction via carbon nanotubes, ionic conduction via ionic liquids, and redox transport via redox molecules. Flexible composite materials comprised carbon nanotubes and poly(imidazolium) with allyl and redox pendant groups were fabricated and examined. They demonstrated ionic and electrical conductivity and the faradaic response of the redox-polymerized ionic liquid.
Keywords: Redox ionic liquids; Supercapacitors; Scanning electrochemical microscopy

1. Introduction

Flexible energy-storage devices, including flexible lithium-ion batteries and supercapacitors, are currently attracting a great deal of interest for their potential applications in various flexible electronic systems, including roll-up displays and wearable personal multi-media[1]. Endowing flexibility to supercapacitors, which feature long cycling stability, fast charging, and high power density remains subject to challenging developments. Due to their high specific surface area

and excellent mechanical, electrical, and electrochemical properties, carbon nanotubes (CNTs) have been extensively used as electrode materials[2,3]. Their high aspect ratio favors flexibility, besides ensuring continuous conductive paths. However, pseudocapacitive materials that store energy through surface redox reactions exhibit substantially higher specific capacitances than new carbon materials, in which the charge accumulation in the electrical double layer is limited. To further enhance the performance of CNT-based flexible electrical double-layer capacitors (EDLC), composites containing CNT, transition metal oxides, or conductive polymers have been developed to impart pseudocapacitance to the flexible supercapacitors[1,2,4].

Further, polymers are commonly used as flexible electrode materials and flexible solid-state electrolytes[5]. New classes of redox polymers are emerging as electrode materials for batteries (especially organic radical ones)[6]. Unlike conductive polymers (e.g., poly(pyrrole) or poly(aniline)), which demonstrate a floating potential that strongly depends on the polymer's degree of doping, which varies upon charging/discharging[7], polymers bearing redox pendant groups (that is well defined electrochemically active groups, typically stable organic radicals), can ensure stable cell voltage[8].

Polymerized ionic liquids (PILs), which combine the properties of both ionic liquids[9,10] and polymeric materials[11], have been developed as electrolytes in various energy devices[12]. They have also been successfully used as a component of composite materials for electrodes, concerning the well-known affinity of imidazolium derivatives and CNTs and reduced graphene oxide[13]. Polyvinylimidazolium-wrapped carbon nanotubes were shown to disperse better in water compared to pristine CNTs and the mixture of ionic liquid monomers and CNTs. They provided promising materials for direct electrochemistry and biosensing of redox proteins by demonstrating superior electrocatalysis performance toward O_2 and H_2O_2[14]. In lithium-ion batteries, polyvinylimidazolium-based binders have been shown to convey the superior electrochemical stability of ILs to cathode materials, demonstrating outstanding long-term cycling durability[15]. Furthermore, literature established another approach to designing high-energy and high-power battery electrodes by hybridizing a nitroxide-polymer redox supercapacitor with a Li-ion battery material[16]. In this paper, we have synthesized and formulated a redox ionic liquid and mixed it with carbon nanotubes to obtain new supercapacitor electrodes (**Figure 1**).

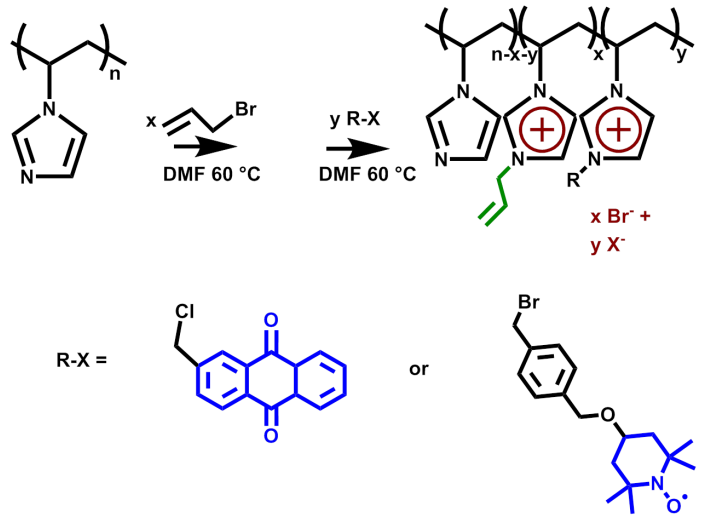

Figure 1. Synthetic route to the cross-linkable redox polyimidazoliums from 2-(chloromethyl)anthraquinone and p-bromomethyl-benzyloxy-2,2,6,6-tetramethyl piperidinyloxy

2. Experimental Section

The chemicals were purchased from Sigma Aldrich, except 1-butyl-3-methylimidazolium bis(trifluoromethylsulfonyl)imide, supplied by Solvionic. They were used as obtained, except 1-vinylimidazole, which was distilled (Eb 88 °C) before being used.

Solvents were purchased from the following suppliers: Dimethylformamide (VWR Chemicals), Acetone (Sigma Aldrich), Methanol (Sigma Aldrich, Chromasolv for HPLC, ⩾ 99,9%).

2.1 Synthesis of Bromomethyl-benzyloxy-2,2,6,6-Tetramethyl piperidinyloxy

A solution of 4-hydroxy-2,2,6,6-Tetramethylpiperidinyloxy (3.0 g, 17.5 mmol) in dry acetone (60 mL) was treated with 60% sodium hydride (0.7 g, 17.5 mmol) while stirring at room temperature. After 10 min of dihydrogen evolution, dibromo-p-xylene (7 g, 26.0 mmol) was added. The resulting mixture was stirred at room temperature for three hours. Under vacuum, the solvent was extracted, resulting in an orange solid. Several milliliters of distilled water were added. The resulting orange aqueous solution was extracted with dichloromethane after the appearance of a white solid, which was filtered off. Before purification by flash chromatography on a silica column with a 90/10 cyclohexane/acetone mixture as the eluent, the organic phase was dried over $MgSO_4$ and evaporated. The final (paramagnetic) product was obtained as an orange oil (21% yield; one only spot observed by thin-layer chromatography).

2.2 Synthesis of Polymerized Ionic Liquids

According to the literature[11], the starting polymer was prepared from 1-vinylimidazol in the presence of azobisisobutyronitrile (AIBN) as a radical initiator. Based on the 1H NMR spectrum (**Figure 2**), the polymerization degree (DP) was estimated to be approximately 400. The thermal properties of the polymer show a Tg at 180°C (**Figures 3 and 4**).

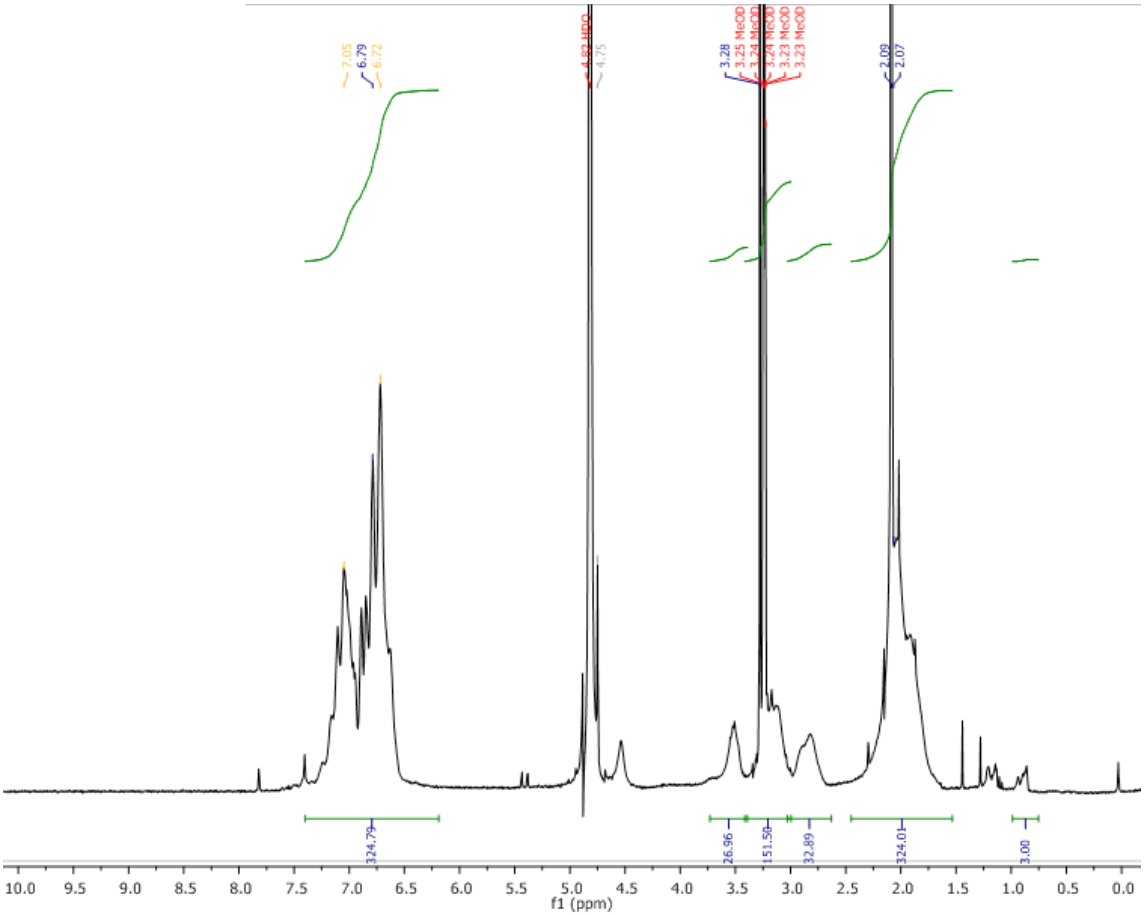

Figure 2. 1H NMR spectrum of poly(1-vinylimidazole)

The NMR of Poly(1-vinylimidazole) is detailled here: ^{1}H NMR (600 MHz, MeOD, δ ppm): 0.97 (m, 6H), 2.07 (m, 4H), 2.90 (m, 1H), 3.19 (m, 1H), 3.62 (m, 1H), 6.81 (m, 2H), 6.94 (m, 2H), 7.14 (m, 1H). ^{13}C NMR (125 MHz, MeOD, δ ppm): 42.25, 53.40, 118.01, 130.43, 137.76.

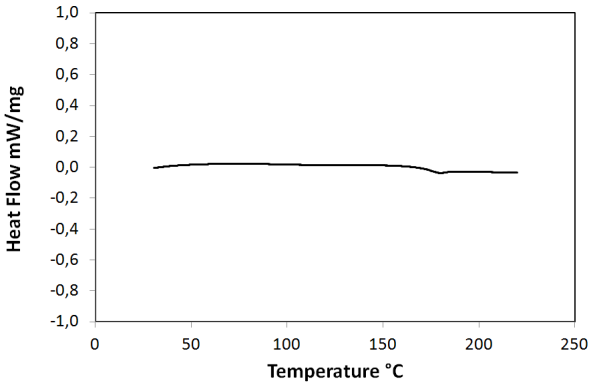

Figure 3. Thermogram of poly(1-vinylimidazole): Tg = 180.3 °C.

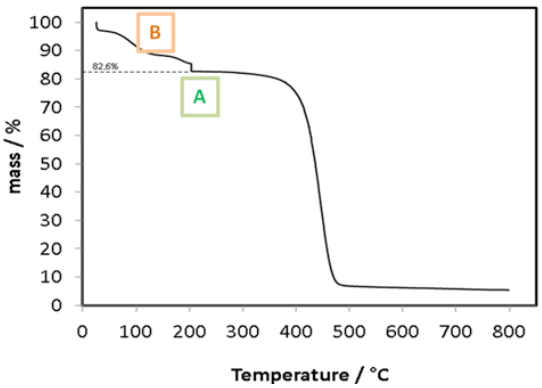

Figure 4. TGA thermogram of poly(1-vinylimidazole): (A) degradation at 458 °C; (B) volatiles (B)

Exchange reactions of the first quaternisation step with allyl bromide: In 150 mL of DMF, 5.00 g of poly(1-vinylimidazole) was dissolved. 575 mg of 1-bromopropene was added to the solution that was obtained. The mixture was heated at 60 °C for twenty-four hours. A solution of orange hue was obtained. The organic layer (1-bromopropene) was subsequently removed, and the aqueous phase was placed in a rotary evaporator at 30 mbar and 65 °C. The obtained solid was then vacuum-dried overnight at 50°C. The substance was orange in color. The detailled NMR is given here: ^{1}H NMR (600 MHz, MeOD, δ ppm): 1.03 (m, 6H), 2.22 (m, 4H), 3.19 (m, 1H), 4.54 (m, 1H), 4.71 (m, 1H), 5.53 (m, 1H), 6.07 (m, 1H), 6.87 (m, 2H), 7.12 (m, 1H) and 7.43 (m, 1H).

The extent was calculated from the area of the multiplet between 6.77 ppm and 7.83 ppm, corresponding to the imidazole ring's three protons, and the broad signal at 6.03 ppm, corresponding to the allyl group's C2 proton (**Figure 5**).

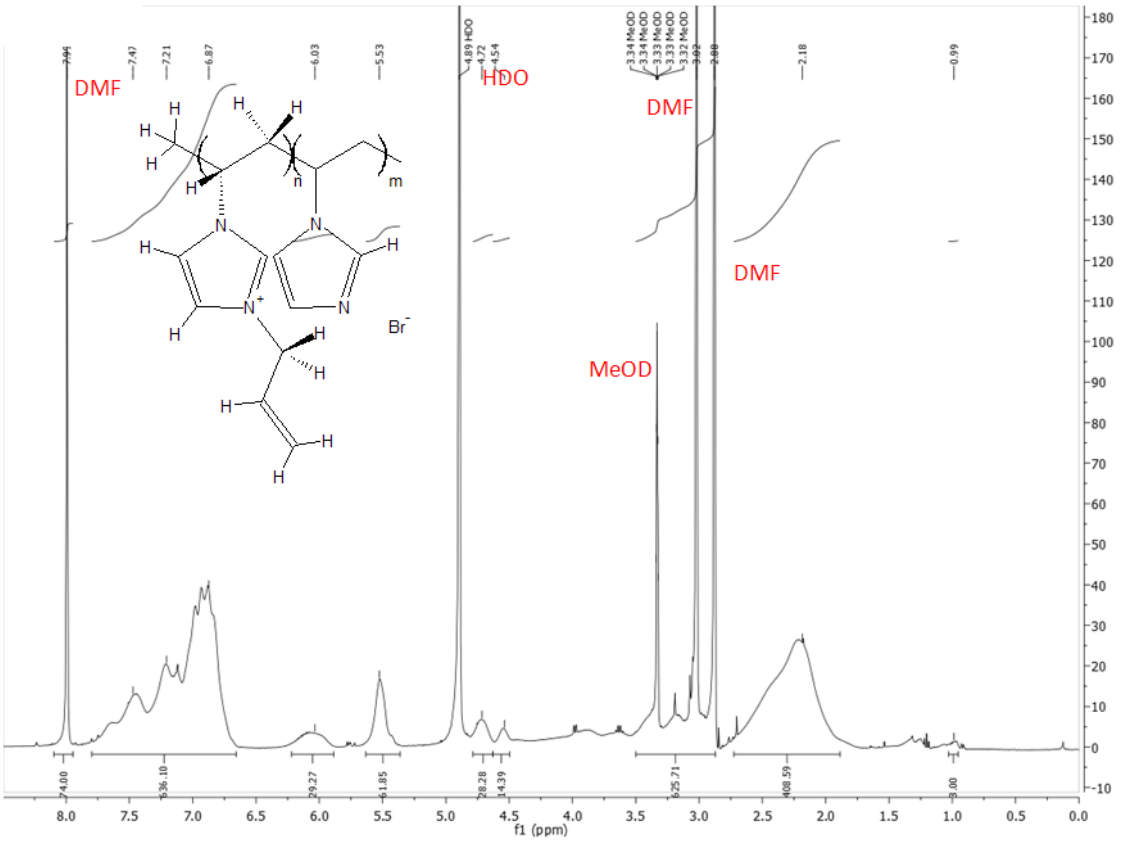

Figure 5. 1H NMR spectrum of allyl functionalized poly(1-vinylimidazolium) bromide

2.3 Anodic Polymerized Ionic liquids

150 mL of MeOH contains 1.32 g of p-bromomethyl-benzyloxy-2,2,6,6-tetramethyl piperidinyloxy and 500 mg of allyl poly(1-vinylimidazole). 24 h at 60 °C heated the reaction mixture. The solution was evaporated at 200 mbar and 40 °C to produce a light orange solid.

Metathesis step: 2.21 g of polymer were dissolved in 50 mL of distilled water. Stirring for 10 min was required for the complete dissolution. The solution was mixed with an aqueous solution of the equimolar amount of Li[TFSI], then strongly stirred for 3 h at room temperature. After extraction with dichloromethane, the polymer was obtained as an orange and viscous liquid.

Figure 6 displays the EPR spectrum of poly(3-allyl-*co*-3-2,2,6,6-tetramethyl piperidinyloxy-1-vinylimidazolium) bis(trifluoromethylsulfonyl) imide in acetonitrile. A calibration curve was drawn with commercial 2,2,6,6-tetramethyl piperidinyloxy (TEMPO) concentrations ranging between 4.10^{-5} M and 8.10^{-4} M (**Figure 6**) and the EPR data is given in **Figure 7**. From measurements on different poly(3-allyl-TEMPO-1-vinylimidazolium) batches, TEMPO content was assessed at around 20%.

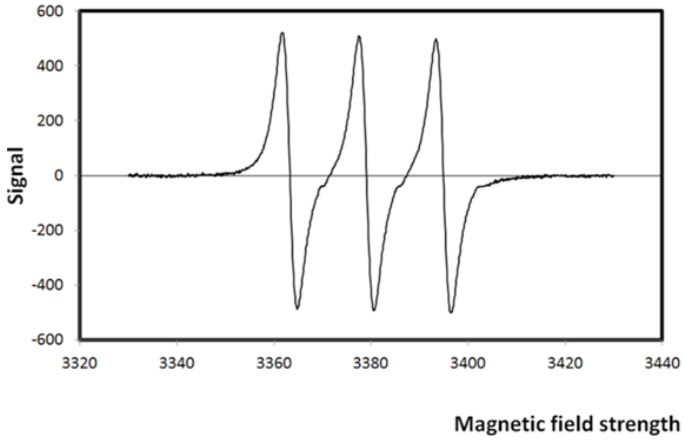

Figure 6. EPR spectrum of poly(3-allyl-*co*-3-TEMPO-1-vinylimidazolium) bis(trifluoromethylsulfonyl)imide

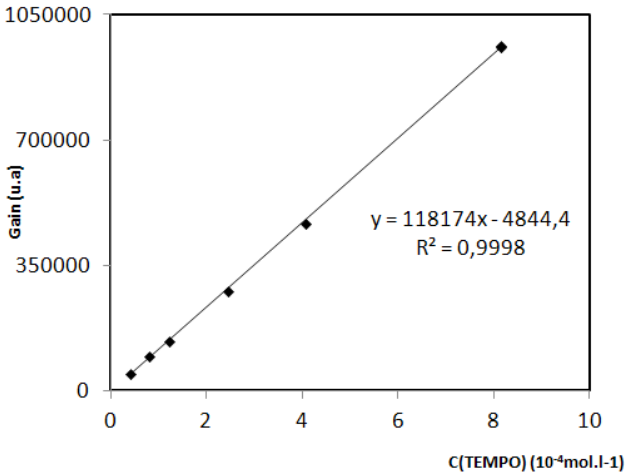

Figure 7. Calibration curve with commercial TEMPO

2.4 Cathodic PILS

Poly(3-allyl-*co*-3-AQ-1-vinylimidazolium) chloride was prepared by using the same procedure with 2-(chloromethyl)anthraquinone. The metathesis step was carried out as above. 3.00 g of poly(3-allyl-AQ-1-vinylimidazolium) chloride were dissolved in 200 mL of acetonitrile. An equimolar amount of Li[TFSI] (2.70 g in 50 mL of acetonitrile) was added into the polymer solution. The reaction mixture was stirred for 3 h at room temperature. The precipitate was removed by filtration and the solution was evaporated, yielding a waxy compound. The NMR is detailled here (**Figure 8**):

1H NMR (600 MHz, MeOD, δ ppm): 2.22 (m, 4H), 3.19 (m, 1H), 4.54 (m, 1H), 4.71 (m, 1H), 5.53 (m, 1H), 6.07 (m, 1H), 6.87 (m, 2H), 7.12 (m, 1H), 7.43 (m, 1H), 8.03 (m, 4H) and 8.44 (m, 4H).

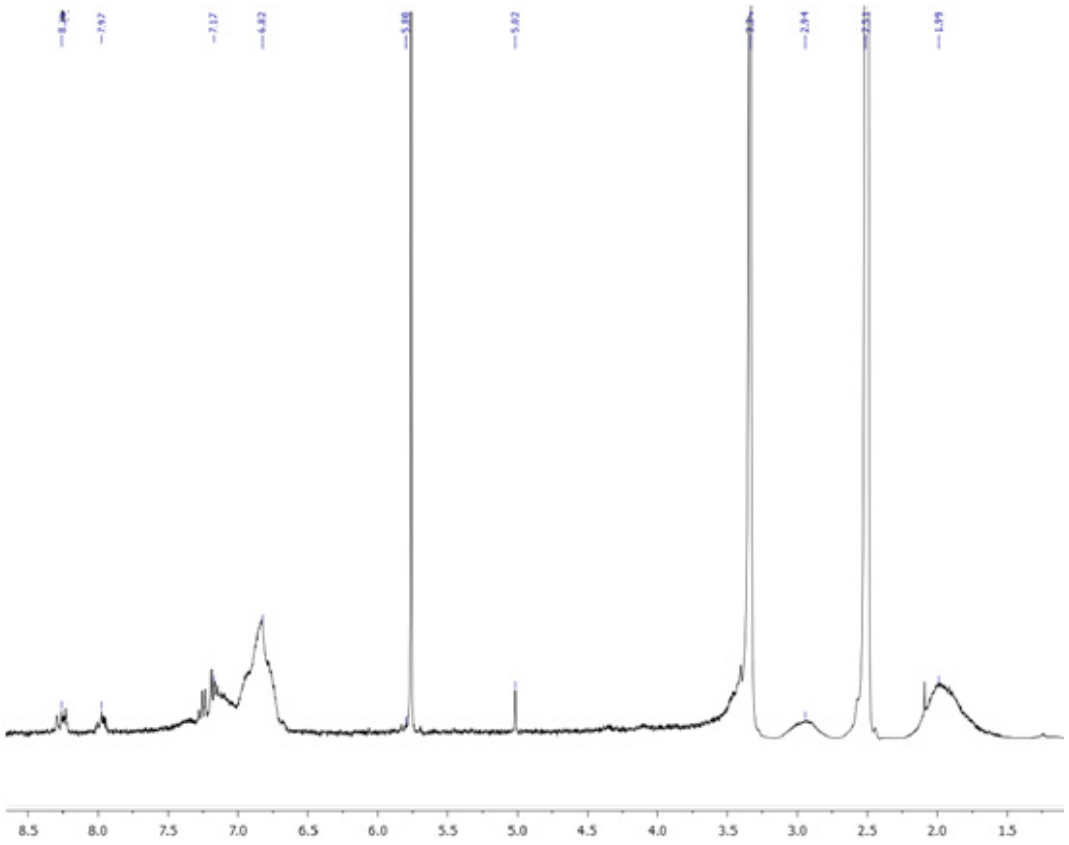

Figure 8. 1H NMR spectrum of poly(3-allyl-*co*-3-AQ-1-vinylimidazolium) bis(trifluoromethylsulfonyl)imide

The extent of quaternisation was estimated at 30% based on the integrations of the multiplets located between 7.97 ppm and 8.44 ppm (AQ = 7 H) and between 6.77 ppm and 7.83 ppm (3 H), respectively.

2.5 Preparation of Multi-Walled Carbon Nanotube (MWCNT) Suspensions

100 mg of PILs were dissolved in 10 mL of MeOH. After complete dissolution, 30 mg of MWCNTs were added, along with 0.01% of photoinitiator (2,2-dimethoxy-2-phenyl acetophenone). The suspension was stirred for 10 min and then submitted to ultrasonication for 15 more minutes.

2.6 Preparation of PILs@CNT and Redox-PILs@CNT Membranes

The above suspension was heated at 45 °C for 20 min to obtain a paste. 15 min of ultrasonication were necessary before casting onto gold disks. Electrodes were obtained after 40 min of irradiation. Irradiation conditions: wavelength 340 nm (radiation source: 3UV tubes that provide a spectral range between 315-400 nm) in the presence of 2,2-dimethoxy-2-phenylacetophenone (DMPA) as a radical initiator. A similar working up was applied for PILs membranes (without MWCNTs).

2.7 Characterizations

2.7.1 NMR

^{1}H and ^{13}C NMR spectra were recorded on a Brücker AVANCE III 600 instrument. Different deuterated solvents were used according to the solubility of the compounds at room temperature. The values of chemical shifts are expressed in ppm and referenced to TMS. The multiplicity of the signals is indicated by the following abbreviations: s (singlet), d (doublet), t (triplet), and m (multiplet).

2.7.2 Thermal analyses

Thermal gravimetric analyses were carried out on a Netzsch STA 409 PC apparatus under a nitrogen atmosphere between 25 °C and 700 °C at a heating rate of 5 °C/min using ca. 10 mg samples in alumina

crucible.

Differential scanning calorimetry measurements were carried out on a NETSCH DSC 204-F1 apparatus. DSC thermograms were recorded on raising the temperature from -120 °C to 150 °C at a heating rate of 10 °C/min under nitrogen atmosphere.

2.7.3 EPR

The EPR measurements were performed on capillary using a Brüker Elexsys E500 spectrometer in X-CW band (9.5 GHz; power = 1.0 mW; gain = 10 dB).

2.7.4 Cyclic voltammetry and scanning electrochemical microscopy

Electrochemical measurements were carried out on a Biologic VMP3 potentiostat operating under EC-Lab V10.38 software. Cyclic voltammetry experiments were conducted using a symmetric Swageloks-type two-electrode cell with PILs@CNT or redox-PILs@CNT material at both positive and negative electrodes. A glass microfiber Whatman filter paper (thickness 260 µm and pore diameter 1.6 µm) was utilized as the separator. Cyclic voltammetry was performed in a potential window of 2.8 V with scan rates from 5 mV/s to 200 mV/s.

3. Results and Discussions

Combining the properties of polymerized ionic liquids and redox polymers to create new processable polymers was the driving force behind this study. To our knowledge, the polyvinylimidazoliums reported here are the first examples of redox PILs. Thus, polyvinylimidazole chains[17] were randomly functionalized by successive quaternization reactions with cross-linkable groups (allyl) and redox groups, specifically anthraquinone (cathode material) or 2,2,6,6-tetramethylpiperidinyloxy (TEMPO; anode material) **(Figure 1**).

The first quaternization reaction was limited to about 14% of the imidazole units using a sub-stoichiometric amount of allyl bromide. The second quaternization reactions were carried out in the presence of excess 2-(chloromethyl)anthraquinone (commercially available) or *p*-bromomethyl-benzyloxy-TEMPO (prepared from α,α'-dibromo-p-xylene, and commercially available 4-hydroxy-TEMPO)[11]. The halide anions were further exchanged for bis(trifluoromethanesulfonyl)imide (TFSI) by metathesis reaction with Li[TFSI]. The resulting redox polyimidazoliums turned out to be liquid or waxy compounds soluble in methanol. These polymerized ionic liquids were characterized by ^{1}H NMR (anthraquinone derivative) or EPR (TEMPO derivative). The ratio of redox units after the second quaternization step was assessed at only about 30%, despite the activated benzylic position of the electrophilic carbon centers in the halide derivatives. As a benchmark, a non-redox polymerized ionic liquid was synthesized using butyl bromide instead of the redox precursor in the second quaternization step. In this instance, the extent of the quaternization reaction was 100 percent, most likely due to the butyl group's lesser steric hindrance.

Photoactivated cross-linking of the liquids (**Figure 9A**) in the presence of 2,2-dimethoxy-phenylacetophenone (DMPA) as a photoinitiator led to flexible materials (**Figure 9B**). Further, ultrasonic dispersions of MWCNTs in methanol were found to be efficiently stabilized in the presence of the polymers, likely as a result of the presence of imidazolium pendant groups along the polyvinyl main chain[18].

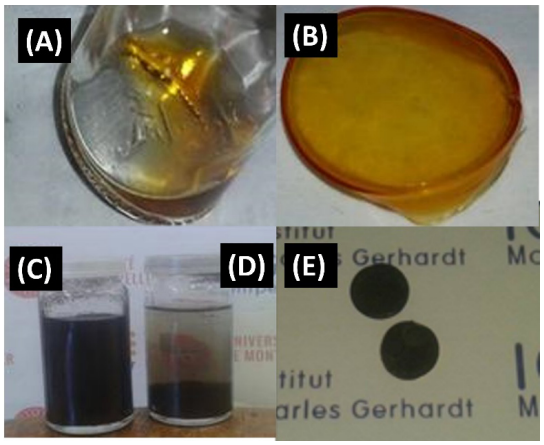

Figure 9. Redox PIL before (A) and after photoactivated cross-linking (B); Suspensions of MWCNTs in methanol with (C) and without (D) redox PIL after 24 h (C) and MWCNT-containing composite membrane after photoactivated cross-linking (E)

As a matter of fact, applying the photoactivated cross-linking on a suspension of MWCNTs in methanol (**Figure 9D**) led to flexible composite PILs@CNT or redox-PILs@CNT membranes (**Figure 9E**). Scanning electron micrographs of composite materials are displayed in **Figure 10**. They disclosed a composite nanostructure corresponding to MWCT bundles intimately embedded in the polymer and forming a

percolating network, as confirmed by the electron conduction ability of the material.

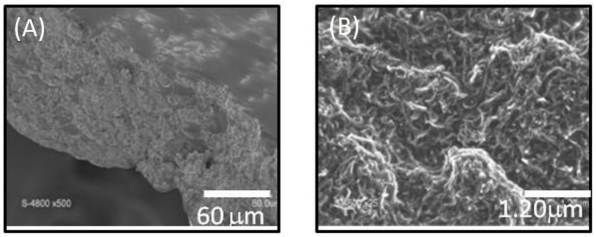

Figure 10. Scanning electron micrographs of a composite redox-PILs@CNT membrane: (A) cross-section; (B) surface

Nyquist diagram shows that the composite based on PILS@CNT has a low resistance (30 Ohms given by fit analysis). This result comes from CNT and induces electronic conduction (**Figure 11**).

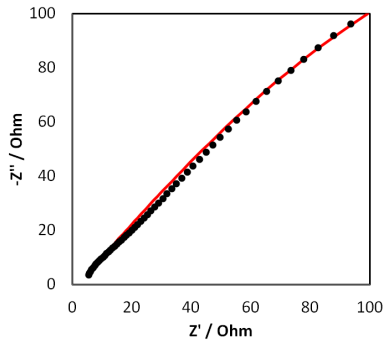

Figure 11. Measured Nyquist diagram of PILs@CNT. Frequency range from 100 kHz to 10 mHz. Red curve is the fit, and the black point are experimental curve

Cyclic voltammetry with anthraquinone-PILs (poly(3-allyl-*co*-3AQ-1-vinylimidazolium) bis(trifluoromethylsulfonyl)imide) or TEMPO-PILs (poly(3-allyl-*co*-3-TEMPO-1-vinylimidazolium) bis(trifluoromethylsulfonyl)imide)) in acetonitrile (**Figure 12** (scan rate of 0.1 V/s)). Almost peak shape was observed, which evidenced the electrochemical response of TEMPO and Anthraquinone. This encouraging result demonstrates that these redox polymer composites can greatly improve composite electrodes.

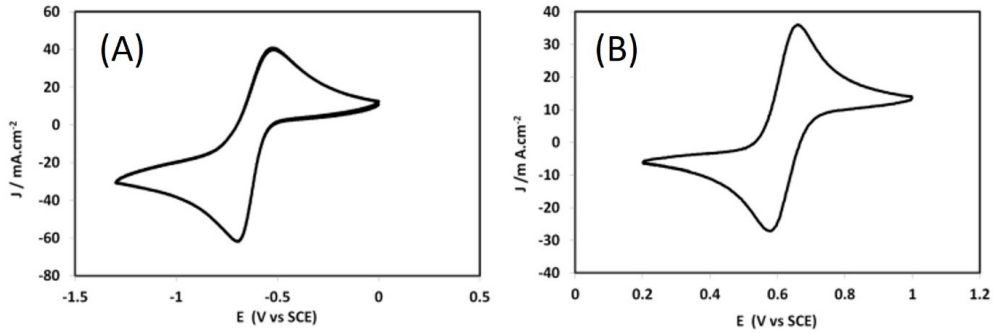

Figure 12. Voltammograms of poly(3-allyl-*co*-3AQ-1-vinylimidazolium) and poly(3-allyl-*co*-3-TEMPO-1-vinylimidazolium) bis(trifluoromethylsulfonyl)imides in acetonitrile at 100 mV/s

Cyclic voltammetry with PILs@CNT or redox-PILs@CNT as electrodes and 1-butyl-3-methylimidazolium bis(trifluoromethylsulphonyl)imide [BMIm][TFSI] as an electrolyte is shown in **Figure 13** (scan rate of 0.1 V/s). An almost rectangular shape (without redox peaks) was observed for PILs@CNT, which evidenced the electrochemical double-layer capacitance of MWCNTs in the composite. In contrast, when using redox-PILs@CNT as electrodes, broad redox peaks were observed, which could be attributed to the introduction

of TEMPO and anthraquinone moieties on positive and negative electrodes, respectively. The electrode-specific capacitance of the supercapacitors with PILs@CNT and redox-PILs@CNT were determined to be 142 F/g (a good value regarding the literature[9,19]) and 346 F/g, respectively. This encouraging result indicates that this type of redox polymer composite can significantly enhance the capacitive properties of supercapacitors via the pseudocapacitive effect.

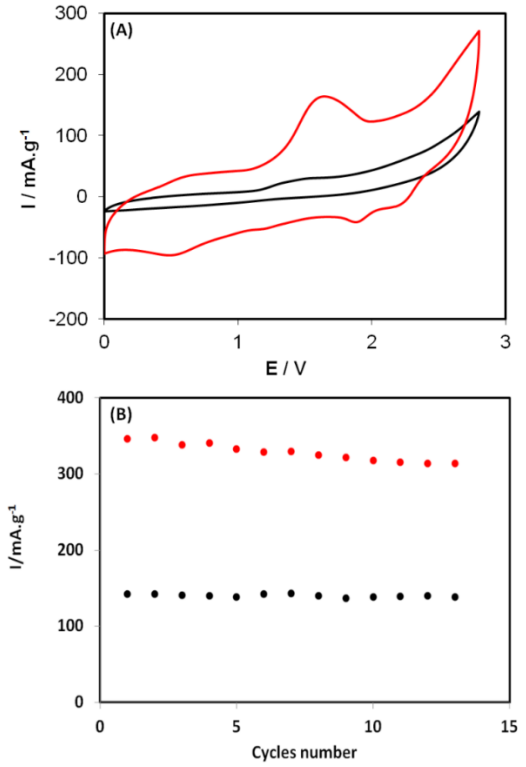

Figure 13. (A) Two-electrodes cyclic voltammetry of PILs@CNT (black line) and redox-PILs@CNT (red line) membranes (electrolyte [BMIm][TFSI]; scanning rate 0.1 V/s); (B) Capacitance retention upon cycling in redox-PILS@CNT (in red and full scatter) vs. PILS@CNT (in blue and empty scatter) for symmetric devices

To further investigate electrochemistry, we carried out an approach curve measurement by SECM of the electrode material. SECM is a technique that allows the analysis of the kinetics at the interface of an electrode and a redox molecule, the probe.

Bard and co-workers founded SECM in the 1980s. SECM uses an ultramicroelectrode (UME) to probe three-dimensional surfaces (**Figure 14**). By moving the UME, different areas on the same surface can be studied, and an electrochemical image can be obtained by scanning in x and y. The UME allows local studies of surfaces' electrochemical properties, such as the composite electrodes in this study. Surface information is obtained by disturbing the UME's current register. In feedback mode, UME is immersed in a redox mediator solution (i.e., an electroactive species). The tip approaches the surface while a constant potential is applied. The type of surface and solution species affect the UME response current when the tip is close. The approach curve is given in **Figure 14A**. The approach curves are usually represented by plotting the current at the tip. There are two types of limiting cases: positive feedback and negative feedback. When the UME is brought close to the insulator, the species generated at the UME are incapable of reacting with an insulating surface, such as a glass substrate. A potentiostat can control the rate of the reaction that is taking place on the surface if the surface itself is a conductor—normalized by the current far from the surface ($I_t = i_t/i_{inf}$) in the function of the tip-surface distance normalized by the UME radius (L = d/a).

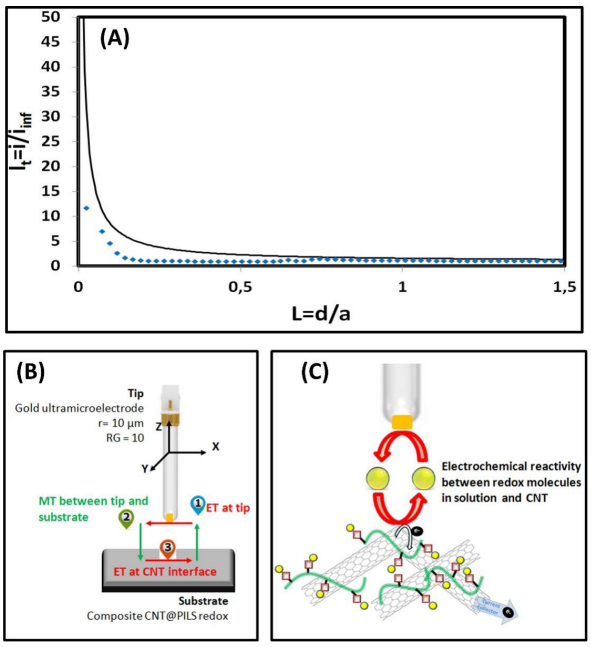

Figure 14. Scanning electrochemical microscopy measure. (A) SECM approach curves at a Pt disk UME tip (radius: 5 µm) on composite CNT@PILs redox TEMPO; (B) and (C) Illustration of the reactivity at the interface

There are two limiting cases called negative feedback and positive feedback. When the UME has approached an insulating surface, such as a glass substrate, the

species generated at the UME cannot react at the insulator. If the surface is a conductor, the reaction rate on the surface can be controlled by the potentiostat. The approach curves depend on the rate constant (k_{app}) for electron transfer between the electrogenerated mediator and the surface. For an insulator, $k_{app} \rightarrow 0$, and for a conductor, $k_{app} \rightarrow \infty$. In the space between these two extreme cases, an intermediate value of k_{app} can be found. In this instance, the analysis of SECM reveals positive feedback, which indicates that the composite in question is highly conductive and that the kinetic energy associated with the transfer of electrons is elevated.

So, the SECM method allows seeing the electronic conduction of the electrode material (here, the CNT/PILS composite), as shown in **Figures 14B and 14C**. In our case, the redox probe is a free TEMPO molecule in solution, which reacts at the interface of the composite electrode. As it reacts at the electrode interface, the current measured on the tip increases. This signature is called positive feedback, and thus proves the conductive character of the composite material.

4. Conclusions

New polyvinylimidazoliums bearing both cross-linkable and redox side-groups along the main chain have been prepared. Liquid and soluble, they demonstrated to be easily processable, and, moreover, turned out to efficiently stabilize dispersions of MWCNTs in alcohol. Accordingly, flexible conducting composite materials were implemented by photoactivated cross-linking. As revealed by SEM, the polymers turned out to be excellent binders. Composite materials comprising TEMPO and anthraquinone moieties were applied to supercapacitors, as positive and negative electrode materials, respectively. Preliminary tests disclosed a significant Faradic contribution to energy storage, which resulted in capacitances twice as high as the parent material derived from PILs without redox groups. Redox polyvinylimidazoliums bearing cross-linkable groups appear as a promising new family of PILs for designing high-performance electrode materials for flexible electrochemical devices.

References

[1] Wang X, Lu X, Liu B, *et al*. Flexible energy-storage devices: design consideration and recent progress. *Advanced Materials*, 2014;26(28):4763-4782. https://doi.org/10.1002/adma.201400910

[2] Chen T and Dai L. Flexible supercapacitors based on carbon nanomaterials. *Journal of Materials Chemistry A*, 2014;2(28):10756-10775. https://doi.org/10.1039/C4TA00567H

[3] Li RQ, Zeng S, Sang B, *et al*. Regulating electronic structure of porous nickel nitride nanosheet arrays by cerium doping for energy-saving hydrogen production coupling hydrazine oxidation. *Nano Research*, 2022:1-8. https://doi.org/10.1007/s12274-022-4912-3

[4] Mourad E and Fontaine O. Redox bucky gels: mixture of carbon nanotubes and room temperature redox ionic liquids. *Journal of Materials Chemistry A*, 2019;7(21):13382-13388. https://doi.org/10.1039/C9TA01359H

[5] Snook GA, Kao P and Best AS. Conducting-polymer-based supercapacitor devices and electrodes. *Journal of Power Sources*, 2011;196(1):1-12. https://doi.org/10.1016/j.jpowsour.2010.06.084

[6] Gracia R and Mecerreyes D. Polymers with redox properties: materials for batteries, biosensors and more. *Polymer Chemistry*, 2013;4(7):2206-2214. https://doi.org/10.1039/C3PY21118E

[7] Shown I, Ganguly A, Chen LC, *et al*. Conducting polymer-based flexible supercapacitor. *Energy Science & Engineering*, 2015;3(1):2-26. https://doi.org/10.1002/ese3.50

[8] Janoschka T, Hager MD and Schubert US. Powering up the future: radical polymers for battery applications. *Advanced Materials*, 2012;24(48):6397-6409. https://doi.org/10.1002/adma.201203119

[9] Wei D and Ng TW. Application of novel room temperature ionic liquids in flexible supercapacitors. *Electrochemistry Communications*, 2009;11(10):1996-1999. https://doi.org/10.1016/j.elecom.2009.08.037

[10] Mourad E, Coustan L, Lannelongue P, *et al*. Biredox ionic liquids with solid-like redox density in the liquid state for high-energy supercapacitors. *Nature Materials*, 2017;16(4):446-453. https://doi.org/10.1038/nmat4808

[11] Chen H and Elabd YA. Polymerized ionic liquids: solution properties and electrospinning.

Macromolecules, 2009;42(9):3368-3373. https://doi.org/10.1021/ma802347t

[12] Qiu B, Lin B and Yan F. Ionic liquid/poly (ionic liquid)-based electrolytes for energy devices. *Polymer International*, 2013;62(3):335-337. https://doi.org/10.1002/pi.4454

[13] Fukushima T and Aida T. Ionic liquids for soft functional materials with carbon nanotubes. *Chemistry-A European Journal*, 2007;13(18):5048-5058. https://doi.org/10.1002/chem.200700554

[14] Xiao C, Chu X, Wu B, *et al*. Polymerized ionic liquid-wrapped carbon nanotubes: the promising composites for direct electrochemistry and biosensing of redox protein. *Talanta*, 2010;80(5):1719-1724. https://doi.org/10.1016/j.talanta.2009.10.012

[15] Yuan J, Prescher S, Sakaushi K, *et al*. Novel polyvinylimidazolium nanoparticles as high-performance binders for lithium-ion batteries. *Journal of Materials Chemistry A*, 2015;3(14):7229-7234. https://doi.org/10.1039/C5TA01374G

[16] Vlad A, Singh N, Rolland J, *et al*. Hybrid supercapacitor-battery materials for fast electrochemical charge storage. *Scientific Reports*, 2014;4(1):1-7. https://doi.org/10.1038/srep04315

[17] Yuan J, Márquez AG, Reinacher J, *et al*. Nitrogen-doped carbon fibers and membranes by carbonization of electrospun poly(ionic liquid)s. *Polymer Chemistry*, 2011;2(8):1654-1657. https://doi.org/10.1039/C1PY00196E

[18] Soll S, Antonietti M and Yuan J. Double stimuli-responsive copolymer stabilizers for multiwalled carbon nanotubes. *ACS Macro Letters*, 2012;1(1):84-87. https://doi.org/10.1021/mz200042h

[19] Kang YJ, Chung H, Han CH, *et al*. All-solid-state flexible supercapacitors based on papers coated with carbon nanotubes and ionic-liquid-based gel electrolytes. *Nanotechnology*, 2012;23(6):065401. https://doi.org/10.1088/0957-4484/23/6/065401